THE FASEB JOURNAL • RESEARCH • www.fasebj.org

The dynamic adaptation of primary human endothelial cells to simulated microgravity

Alessandra Cazzaniga,[1] Laura Locatelli,[1] Sara Castiglioni, and Jeanette A. M. Maier[2]
Dipartimento di Scienze Biomediche e Cliniche L. Sacco, Università di Milano, Milano, Italy

ABSTRACT: Culture of human endothelial cells for 10 d in real microgravity onboard the International Space Station modulated more than 1000 genes, some of which are involved in stress response. On Earth, 24 h after exposure to simulated microgravity, endothelial cells up-regulate heat shock protein (HSP) 70. To capture a broad view of endothelial stress response to gravitational unloading, we cultured primary human endothelial cells for 4 and 10 d in the rotating wall vessel, a U.S. National Aeronautics and Space Administration–developed surrogate system for benchtop microgravity research on Earth. We highlight the crucial role of the early increase of HSP70 because its silencing markedly impairs cell survival. Once HSP70 up-regulation fades away after 4 d of simulated microgravity, a complex and articulated increase of various stress proteins (sirtuin 2, paraoxonase 2, superoxide dismutase 2, p21, HSP27, and phosphorylated HSP27, all endowed with cytoprotective properties) occurs and counterbalances the up-regulation of the pro-oxidant thioredoxin interacting protein (TXNIP). Interestingly, TXNIP was the most overexpressed transcript in endothelial cells after spaceflight. We conclude that HSP70 up-regulation sustains the initial adaptive response of endothelial cells to mechanical unloading and drives them toward the acquisition of a novel phenotype that maintains cell viability and function through the sequential involvement of different stress proteins.—Cazzaniga, A., Locatelli, L., Castiglioni, S., Maier, J. A. M. The dynamic adaptation of primary human endothelial cells to simulated microgravity. FASEB J. 33, 5957–5966 (2019). www.fasebj.org

KEY WORDS: HUVEC · RWV · stress response

The importance of human exploration of space has been underscored by many successful missions over the past 50 yr. With the increased duration of these missions, it has become evident that space affects the health of astronauts. Space represents a unique environment where various hazardous stimuli coexist. Besides radiation, microgravity importantly contributes to activating an adaptive response, which might be beneficial in space but might exert detrimental effects on tissues and cells when returning to Earth (1). To get insights into the cellular and molecular events involved in human adaptation to weightlessness, many human cell types have been studied in real or simulated microgravity (1). It is now clear that mammalian cells sense alterations of gravity as a stressful event and turn physical cues into biochemical signals, which reprogram their activities (2).

Endothelial cells (ECs), crucial for the integrity of the vascular wall, are very sensitive to mechanical hints (3). In response to different hemodynamic forces, such as fluid shear stress and blood pressure, ECs convert mechanical forces into various biochemical signals, which govern endothelial function and vascular remodeling. Just after the beginning of space missions, it became evident that another physical force (*i.e.*, gravity) is important in regulating endothelial behavior (1). Similar to what happens in response to disturbed shear stress or high blood pressure, gravitational unloading impairs endothelial homeostasis, and this has a role in the onset of spaceflight-associated cardiovascular deconditioning (4). Several studies have investigated the impact of simulated and real microgravity on the function of primary human ECs (5). In particular, the HUVEC is a consolidated model of macrovascular ECs, because HUVEC gene expression clusters tightly with that of other large-vessel ECs (6). In HUVECs, simulated microgravity remodels the cytoskeleton, modulates cell proliferation and cytokine expression, enhances NO production, and up-regulates heat shock protein (HSP) 70 (7–11). Under normal conditions, HSP70 is barely detectable, whereas in response to cellular stress, HSP70 is rapidly up-regulated. In addition to serving as a chaperonin, HSP70 protects ECs from apoptosis by interfering with

ABBREVIATIONS: CDKN1A, cyclin-dependent kinase inhibitor 1A; CTR, static 1 *g* conditions; DCFH, 2′-7′-dichlorofluorescein diacetate; EC, endothelial cell; GAPDH, glyceraldehyde-3-phosphate dehydrogenase; GSH, reduced glutathione; GSSG, oxidized glutathione; HSP, heat shock protein; ICAM-1, intercellular adhesion molecule 1; P-HSP27, phosphorylated HSP27; PON2, paraoxonase 2; ROS, reactive oxygen species; RWV, rotating wall vessel; siRNA, small interfering RNA; SIRT2, sirtuin 2; SOD2, superoxide dismutase 2; SPHINX, Spaceflight of HUVECs, Integrated Experiment; TXNIP, TXR interacting protein; TXR, thioredoxin

[1] These authors contributed equally to this work.

[2] Correspondence: Dipartimento di Scienze Biomediche e Cliniche L. Sacco, Università di Milano, Via GB Grassi 74, 20157 Milano, Italy. E-mail: jeanette.maier@unimi.it

doi: 10.1096/fj.201801586RR

key apoptotic proteins (12), and, accordingly, no apoptosis was detected in HUVECs in simulated microgravity (13). However, it is not yet known if HSP70 up-regulation is directly implicated in preventing cell death in simulated microgravity.

All of these results have been obtained using both the rotating wall vessel (RWV) and the random positioning machine to simulate microgravity for times ranging between 4 and 96 h. These surrogate systems for benchtop microgravity research reduce the average gravitational force acting on the cells to about 10^{-2}–10^{-3} g (8). It is noteworthy that culture of HUVECs, human microvascular ECs, and U937 cells either in the RVW or in the random positioning machine yielded similar results (8, 14, 15). In the case of U937 cells, data obtained in these bioreactors reflect the findings obtained in true microgravity (16).

Two experiments on HUVECs have been performed in space (17–19). The first one lasted 12 d, and the cells displayed profound cytoskeletal alterations, reduced metabolic activity, and increased permeability, which were not reversible upon return to Earth (17, 18). In "Spaceflight of HUVEC: an Integrated Experiment (SPHINX)" (19), HUVECs were cultured for 10 d on the International Space Station. Postflight analysis demonstrated that spaceflight modulates the expression of more than 1000 genes (19), among which the most overexpressed is thioredoxin interacting protein (TXNIP) (19), a stress-responsive gene encoding a protein that contrasts the antioxidant action of thioredoxin (TXR). Currently, no data are available about TXNIP expression in HUVECs in simulated microgravity.

In this work, we aim to define HUVEC stress response after 4 and 10 d of culture in the RWV. Four days is the maximal time length utilized in simulated microgravity, whereas 10 d corresponds to the duration of SPHINX. Moreover, because experiments in space are demanding and subject to several restraints, including the difficulty of culturing enough cells to perform quantitative studies at the protein level, we here extend previous studies limited to gene expression to the assessment of the proteins.

MATERIALS AND METHODS

Cell culture

HUVECs were from the American Type Culture Collection (Manassas, VA, USA) and serially passaged in M199 containing 10% fetal bovine serum, 150 μg/ml EC growth factor, 2 mM glutamine, 1 mM sodium pyruvate, and 5 U/ml heparin on 2% gelatin-coated dishes. The cells were routinely tested for the expression of endothelial markers and used for 5–6 passages. All culture reagents were from Thermo Fisher Scientific (Waltham, MA, USA). To generate microgravity, we utilized the RWV (Synthecon, Houston, TX, USA) after seeding on beads (Cytodex 3; MilliporeSigma, Burlington, MA, USA) (7, 8, 20). As controls, HUVECs grown on beads were cultured in the vessels not undergoing rotation. By 3-[4,5-dimethylthiazole-2-*yl*]-2,5-diphenyltetrazolium bromide assay, HUVECs cultured in static 1 g conditions (CTR) and RWV-cultured HUVECs are viable after 4 and 10 d (unpublished results). In addition, the cells were trypsinized, stained with trypan blue solution (0, 4%), and counted using a Luna Automated Cell Counter (Logos Biosystems, Anyang, South Korea). After 4 d, a 2-fold induction was observed in HUVECs cultured in the RWV *vs.* their controls (7, 8), but at d 10 the cell number was similar as confluence was reached.

Silencing HSP70

The cells were treated with HSP70 small interfering RNA [siRNA; 1 μg, 5′-TTCAAAGTAAATAAACTTTAA-3′ (Qiagen, Germantown, MD, USA)] and 6 μl HiPerfect Transfection Reagent (Qiagen), according to the manufacturer's recommendations. After 8 h, the siRNA transfection medium was replaced with fresh standard medium, and the cells were transferred into the RWV. After 48 h the cells were trypsinized, stained with trypan blue solution (0.4%), and counted as described above. In parallel, apoptosis was assessed using the Cell Death Detection ELISA photometric enzyme immunoassay (MilliporeSigma), which measures cytoplasmic histone-associated DNA fragments (mono- and oligonucleosomes) in the cytoplasmic fraction of cell lysates (21). The experiment was performed in triplicate 2 times. Data are expressed as means ± SD.

Real-time PCR

Total RNA was extracted by the PureLink RNA Mini Kit (Thermo Fisher Scientific). Single-stranded cDNA was synthesized from 1 μg RNA in a 20-μl final volume using the High-Capacity cDNA Reverse Transcription Kit with RNase inhibitor (Thermo Fisher Scientific), according to the manufacturer's instructions. Real-time PCR was performed in triplicate on the 7500 Fast Real-Time PCR System instrument using TaqMan Gene Expression Assays (Thermo Fisher Scientific). **Table 1** summarizes the primers used. The housekeeping gene glyceraldehyde-3-phosphate dehydrogenase (*GAPDH*) was used as an internal reference gene. Relative changes in gene expression were analyzed by the $2^{-\Delta\Delta Ct}$ method (22). The experiment was performed in triplicate 2 times. Data are expressed as means ± SD.

Reactive oxygen species production, reduced *vs.* oxidized glutathione, and comet assay

Reactive oxygen species (ROS) production was quantified using 2′-7′-dichlorofluorescein diacetate (DCFH) on HUVECs cultured in simulated microgravity for various times. The cells were rapidly transferred into black-bottomed 96-well plates (Greiner Bio-One, Kremsmünster, Austria) and exposed for 30 min to 20 μM DCFH solution. The emission at 529 nm of the DCFH dye was monitored using the Glomax-Multi Detection System (Promega, Madison, WI, USA) (23). The results are the means of 3 independent experiments performed in quadruplicate. Data are shown as percentages of ROS levels in HUVECs cultured in the RWV *vs.* CTR ± SD.

TABLE 1. *List of the primers used for real-time PCR*

Gene	Primer
TXNIP	Hs00197750_m1
SIRT2	Hs00247263_m1
HSPA1A	Hs00197750_m1
CDKN1A	Hs00355782_m1
PON2	Hs00165563_m1
SOD2	Hs00167309_m1
HSPB1	Hs00356629_g1
GAPDH	Hs99999905_m1

Reduced glutathione (GSH) and oxidized glutathione (GSSG) were measured using the GSH/GSSG-Glo Assay (Promega), which is a luminescence-based system, according to the manufacturer's instructions. Data are shown as percentages of GSH/GSSG levels in HUVECs cultured in the RWV *vs.* CTR ± SD.

Comet assay was performed after various times of culture in the RWV. HUVECs were mixed with low-melting-point agarose and spread on pretreated slides, which were dyed, immersed in ice-cold lysis solution (0.01 M Tris-HCl, pH 10; 2.5 M NaCl; 0.1 M EDTA; 0.3 M NaOH; 1% Triton; 10% DMSO), and incubated at 4°C for 60 min. Electrophoresis was conducted in ice-cold running buffer (0.3 M NaOH, 0.001 M EDTA) for 30 min at 300 mA. The slides were then rinsed, fixed in ice-cold methanol for 3 min, dried at room temperature, stained with ethidium bromide, and analyzed with a fluorescence microscope (23).

Protein array

After various times of culture in the RWV or in CTR, conditioned media were collected, and HUVECs were lysed in a buffer containing 50 mM Tris-HCl (pH 8.0), 150 mM NaCl, 1 mM EDTA, and 1% NP-40. Cell extracts (80 μg) were utilized to incubate the membranes on which 26 antibodies against human cell stress-related proteins were spotted in duplicate (R&D Systems, Minneapolis, MN, USA) (22), according to the manufacturer's instructions. Densitometry was performed using ImageJ software (National Institutes of Health, Bethesda, MD, USA). Two separate experiments were performed, and data are expressed as percentages of the fold increase in the signal intensity of RWV *vs.* CTR. Conditioned media were used to incubate the membrane on which 40 antibodies against proteins involved in inflammation were spotted in duplicate (RayBiotech, Norcross, GA, USA). Two separate experiments were performed, and representative blots are shown. According to the ImageJ software, no significant differences were detected in any spot (unpublished results). ELISA was utilized to measure the amounts of intercellular adhesion molecule 1 (ICAM-1) (LifeSpan BioSciences, Seattle, WA, USA), according to the manufacturer's instructions. Data are shown as percentages of ICAM-1 levels in HUVECs cultured in the RWV *vs.* CTR ± SD.

Western blot

HUVECs were lysed in 10 mM Tris-HCl (pH 7.4) containing 3 mM $MgCl_2$, 10 mM NaCl, 0.1% SDS, 0.1% Triton X-100, 0.5 mM EDTA, and protein inhibitors, separated on SDS-PAGE, and transferred to nitrocellulose sheets at 400 mA for 2 h at 4°C. Western analysis was performed using antibodies against HSP70 and cyclin-dependent kinase inhibitor-1 p21 (Santa Cruz Biotechnology, Dallas, TX, USA), TXNIP and paraoxonase 2 (PON2) (Thermo Fisher Scientific), sirtuin 2 (SIRT2) (MilliporeSigma, Vimodrone, Italy), superoxide dismutase 2 (SOD2) (BD Biosciences, San Jose, CA, USA), HSP27 and phosphorylated HSP27 (P-HSP27) (Cell Signaling Technology, Danvers, MA, USA), and GAPDH (Santa Cruz Biotechnology). After extensive washing, secondary antibodies labeled with horseradish peroxidase (GE Healthcare, Waukesha, WI, USA) were used. Immunoreactive proteins were detected by the SuperSignal Chemiluminescence Kit (Thermo Fisher Scientific) (24).

NOS activity

NOS activity was measured in the conditioned media by using the Griess method (25). Briefly, conditioned media were mixed with an equal volume of freshly prepared Griess reagent. The absorbance was measured at 550 nm. The concentrations of nitrites in the samples were determined using a calibration curve generated with standard $NaNO_2$ solutions. The experiment was performed in triplicate and repeated 5 times with similar results. Data are shown as percentages of $NaNO_2$ release in HUVECs cultured in the RWV *vs.* CTR ± SD.

Confocal imaging

After 4 and 10 d in the RWV, HUVECs were trypsinized and cytospun on frosted microscope glasses, fixed in PBS containing 3% paraformaldehyde and 2% sucrose (pH 7.6), permeabilized with 4-(2-hydroxyethyl)-1-piperazineethanesulfonic acid–Triton 1%, incubated with anti-TXNIP immunopurified IgGs overnight at 4°C, and stained with an Alexa Fluor 546 secondary antibody (Thermo Fisher Scientific). Finally, cells were mounted with moviol, and images were acquired using a ×63 objective in oil by an SP8 confocal microscope (Leica Microsystems, Buffalo Grove, IL, USA).

Statistical analysis

Statistical significance was determined using the Student's *t* test and set at a value of $P < 0.05$.

RESULTS

The activation of stress response in HUVECs exposed to simulated microgravity

To have a rapid overview of HUVEC stress response in simulated microgravity, we utilized a protein array specifically tailored for stress proteins. Eighty micrograms of lysates from cells cultured in the RWV for 4 and 10 d were utilized. Out of 26 proteins investigated, HSP70, SIRT2, PON2, SOD2, p21, and P-HSP27 were up-regulated (**Fig. 1**).

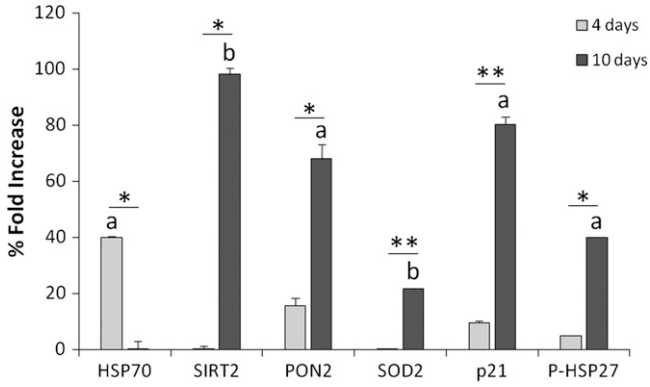

Figure 1. Stress response in HUVECs exposed to simulated microgravity. HUVECs were cultured in the RWV or in CTR for 4 and 10 d. Protein array was performed on cell extracts. Densitometric analysis on array spots was performed, and data are expressed as percentages of the fold increase of the signal intensity obtained in cells in the RWV *vs.* CTR. Different letters (*a*, *b*) indicate the statistically significant effect of RWV *vs.* CTR ($^aP < 0.05$, $^bP < 0.01$). $*P < 0.05$, $**P < 0.01$ (indicates the statistically significant variation of RWV 4 d *vs.* RWV 10 d).

In some cell types, microgravity induces oxidative stress (26–28). Therefore, we measured ROS production by DCFH fluorescence in HUVECs cultured in the RWV for various times. We found a modest, albeit statistically significant, increase of ROS after 2 h in cells in simulated microgravity (RWV) *vs.* CTR and no differences thereafter (**Fig. 2*A***). Because GSH is the most abundant antioxidant in aerobic cells (29), we measured the ratio GSH/GSSG and found it significantly decreased after 2 h in the RWV but not at later times (Fig. 2*B*), thus reinforcing the results obtained using DCFH.

In addition, no oxidative damage of DNA was detected by comet assay (Fig. 2*C*). We propose that the increased amounts of ROS detected after 2 h of culture in the RWV did not reach the threshold to damage DNA.

HSP70 in HUVECs exposed to simulated microgravity

We have previously shown that HSP70 is induced in HUVECs after 24 h of exposure in simulated microgravity and remains elevated up to 96 h (7). In this study, experiments were performed after 4 and 10 d of culture in the RWV. Real-time PCR demonstrates the overexpression of *HSPA1A* (*HSP70*) and Western blot shows the up-regulation of HSP70 (2.1-fold induction) after 4 d of culture in the RWV. Both RNA and proteins return to baseline after 10 d in simulated microgravity (**Fig. 3*A*, *B***).

To understand the role of HSP70 in the early response to simulated microgravity, we transiently silenced *HSP70* using a specific siRNA before exposing HUVECs to gravitational unloading for 48 h. As a control, the cells were exposed to a noninterfering, scrambled sequence. By real-time PCR, *HSP70* expression was down-regulated in silenced HUVECs (Fig. 3*C*). We then counted the cells. As expected (7, 8), HUVECs in the RWV proliferated faster than those in CTR. Silencing *HSP70* completely prevented this effect and cell number was lower than in the controls (Fig. 3*D*). One of the roles of HSP70 is to protect the cells from apoptosis (12). To understand the behavior of HUVEC-silencing *HSP70*, we measured cleaved nucleosomes as an index of apoptosis in HUVECs after 48 h in the RWV using an ELISA. TNF-α (50 ng/ml) was used as a positive control. Figure 3*E* shows that silencing *HSP70* induced the cleavage of

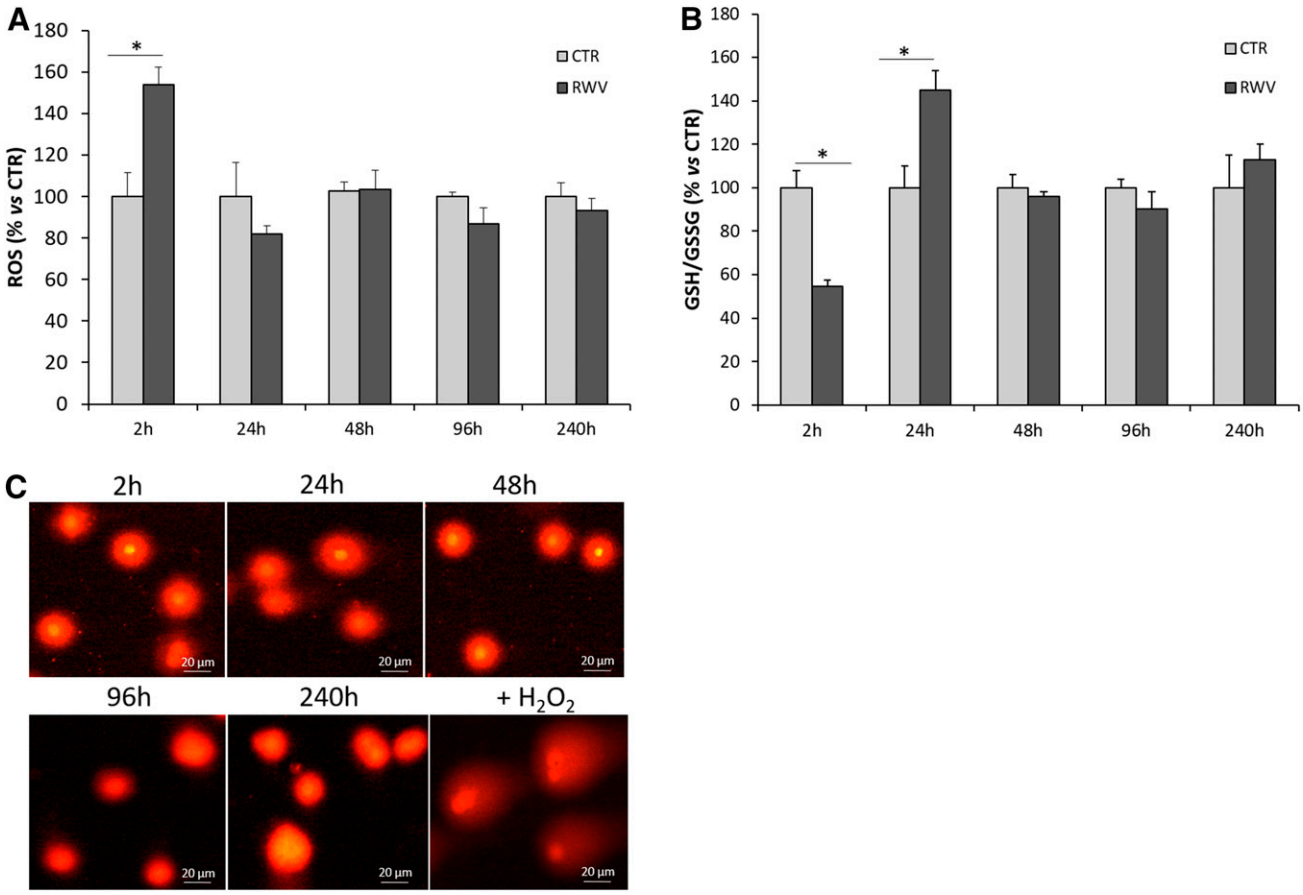

Figure 2. ROS generation, GSH/GSSG ratio, and oxidative damage to DNA in HUVECs exposed to simulated microgravity. HUVECs were cultured for various times in the RWV or in CTR. *A*) ROS generation was measured by DCFH. Data are shown as percentages of ROS levels in HUVECs cultured in the RWV *vs.* CTR. *B*) GSH/GSSG ratio was calculated as described in the Materials and Methods. Data are shown as percentages of GSH/GSSG levels in HUVECs cultured in the RWV *vs.* CTR. *C*) Comet assay was performed. After staining with ethidium bromide, the slides were analyzed using a fluorescence microscope. Exposure to H_2O_2 (100 μM) for 2 h was used as a positive CTR. Scale bars, 20 μm. $^*P < 0.05$.

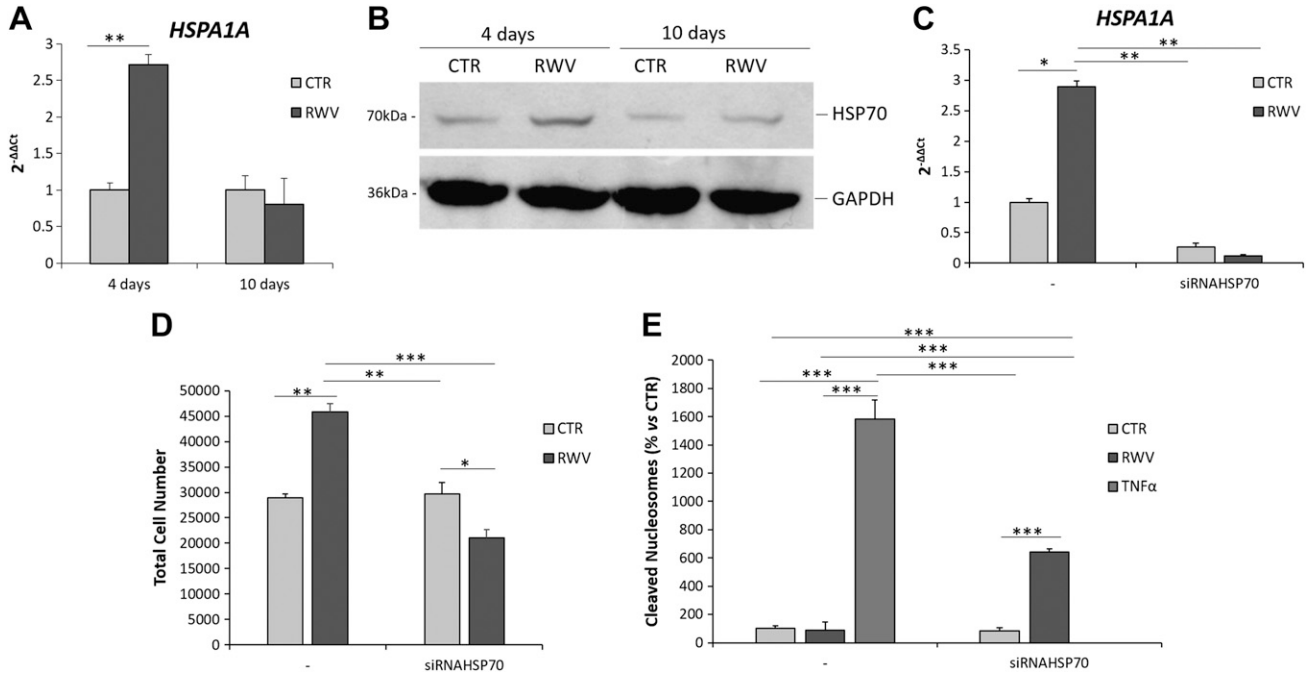

Figure 3. The levels and the role of HSP70 in HUVECs exposed to simulated microgravity. *A*) HUVECs were cultured in the RWV or in CTR for 4 and 10 d. Real-time PCR was performed using primers designed on the *HSPA1A* sequence. The experiment was repeated 3 times in triplicate. *B*) Western blot was performed using specific antibodies against HSP70. GAPDH was used as marker of loading. A representative blot is shown. *C*) HUVECs were transfected with siRNA against *HSP70* or with a scrambled nonsilencing sequence (−) and maintained in the RWV or in CTR for 48 h. To assess silencing, real-time PCR was performed using primers designed on the *HSPA1A* sequence. *D*) Cells treated as in *C* were trypsinized and counted. *E*) Cell death in extracts from HUVECs treated as in *C* was assessed using a Cell Death Detection ELISA Kit, which measures the amount of cleaved DNA and histone complexes. TNF-α (50 ng/ml) for 48 h was the positive CTR. $*P < 0.05$, $**P < 0.01$, $***P < 0.001$.

nucleosomes in HUVECs exposed for 48 h to simulated microgravity.

SIRT2, PON2, SOD2, p21, and HSP27 in HUVECs exposed to simulated microgravity

Next, we examined the levels of the other stress proteins that were increased by protein array. Western blot confirmed that PON2, SOD2, HSP27, and its phosphorylated form are up-regulated after 10, but not 4, d of exposure to simulated microgravity (**Fig. 4*A***). The total amounts of SIRT2 decreased in CTR after 10 d, whereas in HUVECs cultured in the RWV, SIRT2 remained elevated. After 10 d in the RWV, we also detected higher amounts of p21, a cyclin-dependent kinase inhibitor, which also plays a role in stress response (Fig. 4*A*).

It is noteworthy that no significant modulation of *SIRT2*, *PON2*, *SOD2*, and *HSPB1* (*HSP27*) was found by real-time PCR (Fig. 4*B*), thus confirming the results of SPHINX (19). On the contrary, cyclin-dependent kinase inhibitor 1A (*CDKN1A*) (*p21*) was markedly overexpressed after 10 d of culture in the RWV. Our results indicate that *1*) apart from *CDKN1A*, the induction of these proteins is not transcriptionally regulated, and 2) studies limited to gene expression as in Versari *et al.* (19) might hinder our understanding of the complex network of events activated in microgravity.

To understand whether the up-regulation of stress proteins depends on quiescence, which is reached after 8 d in culture (5, 7), we compared the total amounts of SIRT2, PON2, SOD2, HSP70, HSP27, and its phosphorylated form in proliferating *vs.* quiescent HUVECs under physiologic 1 *g* conditions. Whereas SIRT2 was down-regulated and p21 up-regulated in quiescent cells, the other proteins did not change in proliferating *vs.* quiescent cells (Fig. 4*C*). We propose that the up-regulation of PON2, SOD2, HSP70, and HSP27 observed in HUVECs cultured in the RWV is due to gravitational unloading itself.

TXNIP in HUVECs exposed to simulated microgravity

Because *TXNIP* is overexpressed in HUVECs cultured in space (19), we examined the levels of its transcript and the total amounts of the protein by real-time PCR and Western blot, respectively. In agreement with Versari *et al.* (19), we found that *TXNIP* was overexpressed in HUVECs after 10 d in the RWV (**Fig. 5*A***), whereas no modulation of *TXNIP* was detected at d 4 (Fig. 5*A*). Western blot shows that the increase of the RNA correlated with the increase of the protein (2-fold induction at d 10; Fig. 5*B*). Because TXNIP is localized both in the nucleus and in the cytoplasm of HUVECs (30), it is noteworthy that we found the increase of both nuclear and cytosolic TXNIP in HUVECs cultured in the RWV for 10 d by confocal microscopy. No differences emerged after 4 d in simulated microgravity (Fig. 5*C*).

We then compared the total amounts of TXNIP in proliferating *vs.* quiescent HUVECs (Fig. 5*D*) and found

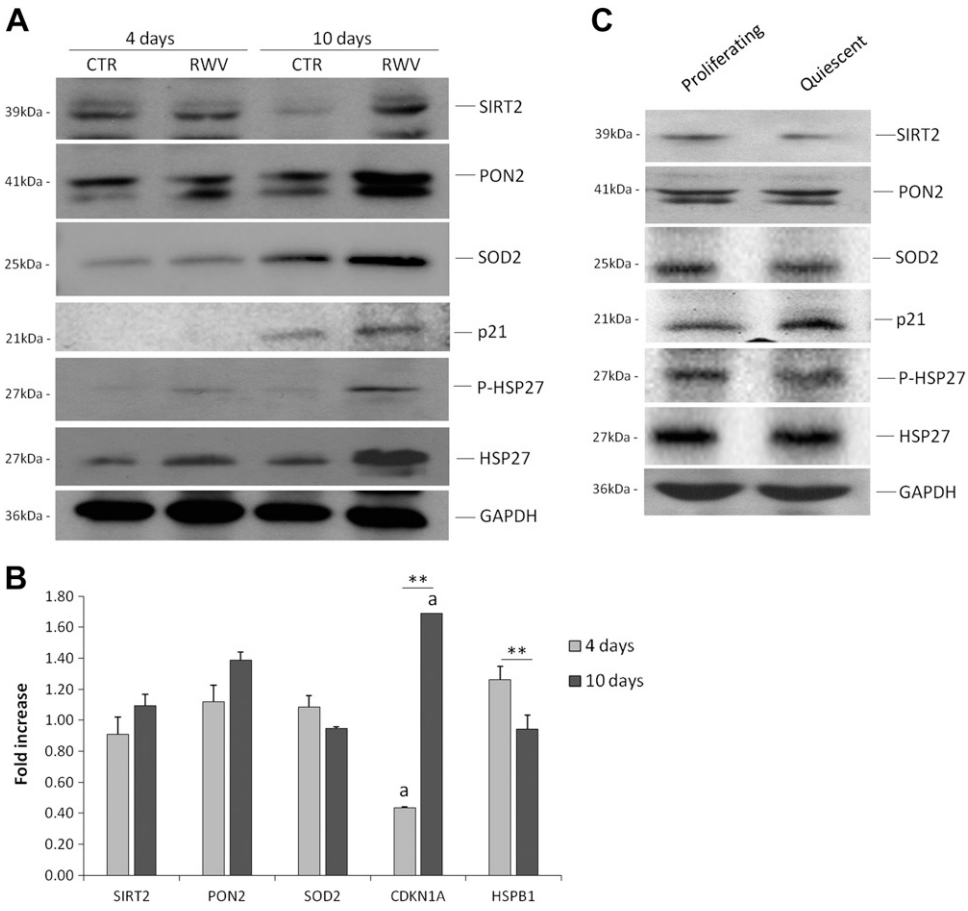

Figure 4. Stress proteins in HUVECs exposed to simulated microgravity. *A*, *B*) HUVECs were cultured in the RWV or in CTR for 4 and 10 d. Western blot and real-time PCR were performed as described in the Materials and Methods. All the values were normalized with respect to their controls cultured in CTR. $^{a}P < 0.05$ (indicates the significant effect of RWV *vs.* CTR). $*P < 0.05$, $**P < 0.01$ (indicates the statistically significant variation of RWV 4 d *vs.* RWV 10 d). *C*) Proliferating and quiescent HUVECs were analyzed for the total amounts of stress proteins by Western blot.

that TXNIP decreases in quiescent cells, thus suggesting that simulated microgravity is directly responsible for the up-regulation of TXNIP after 10 d in RWV.

Endothelial function in HUVECs exposed to simulated microgravity

NO is a multifunctional molecule that influences vascular functions. We have previously shown that HUVECs cultured in simulated microgravity for 24 and 48 h release higher amounts of NO than those cultured in CTR (8). After 4 d of culture in the RWV, HUVECs continued to release more NO than CTR, whereas at d 10, no significant differences were detected (**Fig. 6*A***).

Inflammatory mediators affect endothelial function, and alterations of the cytokine network have been described in ECs exposed to simulated microgravity for 24 and 48 h (7, 9, 20).

In HUVECs cultured in simulated microgravity for 24 and 48 h, a decrease of ICAM-1 was described (9). By ELISA, we did not find any difference in the total amount of ICAM-1 in cells maintained in the RWV for 4 and 10 d (Fig. 6*B*).

To obtain a broad profile of the cytokine network in HUVECs cultured in the RWV for 4 and 10 d, we utilized a human inflammation antibody array. After centrifugation, conditioned media were analyzed. We did not detect any significant alteration in the total amounts of cytokines and chemokines secreted in the conditioned media by HUVECs exposed to simulated microgravity (RWV) *vs.* CTR (Fig. 6*C*, *D*), as confirmed by the ImageJ software (unpublished results).

DISCUSSION

Until now, HUVECs have been cultured in simulated microgravity for various times but not longer than 96 h (5, 7–9). In this study, we focus on the stress response activated by HUVECs exposed to simulated microgravity for 4 and 10 d and demonstrate the crucial early role of HSP70 and the involvement of other stress proteins thereafter.

HSP70 is induced in HUVECs after 24 h of exposure to simulated microgravity (7), is still elevated at d 4, and decreases to baseline at d 10, as suggested by SPHINX (19). We hypothesize that mechanical unloading determines alterations of protein folding, protein aggregation, or both and that this is the trigger for HSP70 up-regulation. Indeed, in HUVECs in microgravity, we and others have reported the early disorganization of the cytoskeleton with the formation of perinuclear clusters of actin (5, 7, 17). HSP70 is thought to participate in folding pathways of cytoskeletal proteins (31). Accordingly, we found that cytoskeletal disruption by cytochalasin D is associated with an increase of HSP70 (unpublished results). We anticipate that the cytoskeleton senses the altered mechanical loading and converts the reduced mechanical stimuli in chemical signals that activate the stress response necessary to maintain the cells' viability. The pivotal role of the

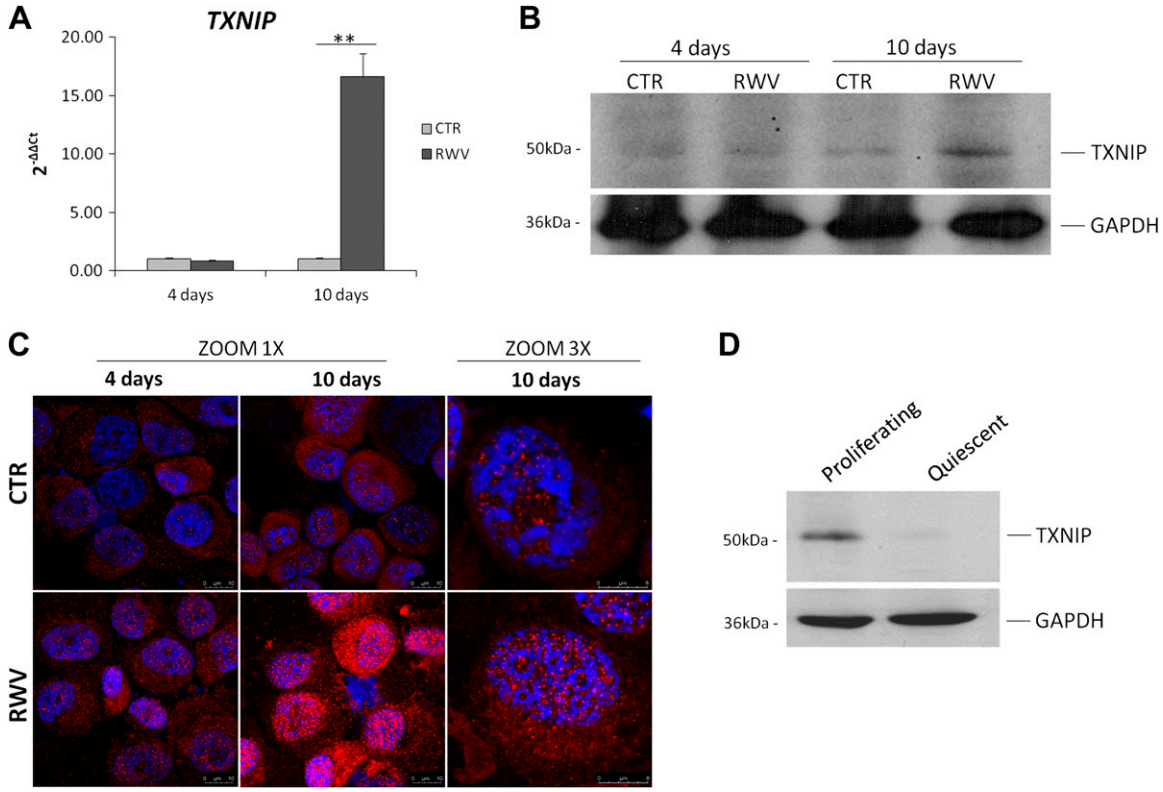

Figure 5. TXNIP in HUVECs exposed to simulated microgravity. *A*, *B*) HUVECs were cultured in the RWV or in CTR for 4 and 10 d. Real-time PCR and Western blot were performed as described in the Materials and Methods. *C*) HUVECs cultured as above were cytospun and stained with DAPI to detect the nuclei and with antibodies against TXNIP. Images were acquired using a ×63 objective in oil by an SP8 confocal microscope (left and center panels, ×1 magnification; right panels, ×3 magnification). *D*) Proliferating and quiescent HUVECs were analyzed for the total amounts of TXNIP by Western blot. $^{**}P < 0.01$.

increase of HSP70 is underlined by the demonstration that silencing *HSP70* induces apoptosis in HUVECs in simulated microgravity. Indeed, HSP70 not only buffers protein misfolding but also inhibits apoptosis acting on caspase-dependent and independent pathways. Altogether, these results indicate that HSP70 is an early gatekeeper for HUVEC

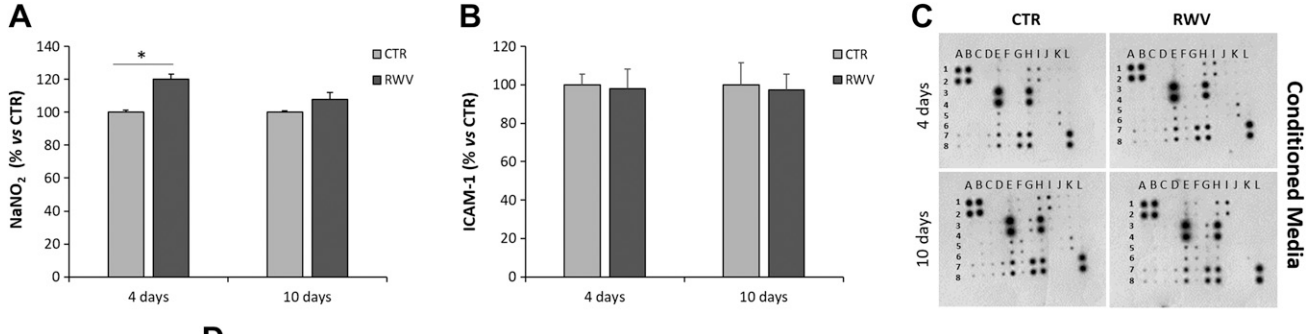

D

	A	B	C	D	E	F	G	H	I	J	K	L
1 2	POS	POS	NEG	NEG	Eotaxin-1	Eotaxin-2	GCSF	GM-CSF	ICAM-1	INF-γ	CCL1	IL-1α
3 4	IL-1β	IL-2	IL-3	IL-4	IL-6	IL-6R	IL-7	IL-8	IL-10	IL-11	IL-12 p40	IL-12 p70
5 6	IL-13	IL-15	IL-16	IL-17 A	IP-10	MCP-1	MCP2	M-CSF	MIG	MIP-1α	MIP-1β	MIP-1δ
7 8	RANTES	TGF-β1	TNFα	TNFβ	TNFRI	TNFRII	PDGF-BB	TIMP-2	BLANK	BLANK	NEG	POS

Figure 6. NO production and inflammatory response in HUVECs exposed to simulated microgravity. HUVECs were cultured in RWV or in CTR for 4 and 10 d. *A*) NO was measured by the Griess method. Data are shown as percentages of $NaNO_2$ release in HUVECs cultured in the RWV *vs.* CTR. *B*) ICAM-1 levels were determined on 80 μg of cell extracts by ELISA. *C*) Inflammatory protein array was performed on conditioned medium. Representative membranes are shown. *D*) Map of the membrane array. $^{*}P < 0.05$.

survival under mechanical unloading. Moreover, HSP70 binds SOD2 in ECs and chaperons it to the mitochondria (32), thus limiting mitochondrial oxidative stress. Accordingly, we did not detect any significant accumulation of ROS in our experimental model.

After 96 h of culture in the RWV, HSP70 returns to basal levels, whereas other stress proteins are up-regulated. Indeed, after 10 d, the amounts of SIRT2, PON2, SOD2, and HSP27 and its phosphorylated form are higher in HUVECs in simulated microgravity than in the 1G conditions. The dysregulation of the anti- and pro-oxidant enzymes we observe in simulated microgravity is not the result of quiescence but seems to be specifically determined by gravitational unloading.

SIRT2, a member of the sirtuin family, is a NAD^+-dependent deacetylase, highly expressed in vascular ECs (33). SIRT2 increases endothelial viability and decreases the levels of ROS by elevating the expression of catalase, glutathione peroxidase, and SOD2 (32). Accordingly, SOD2 is up-regulated in simulated microgravity, and PON2 also increases in HUVECs in the RWV. PON2 is part of the paraxonase family and, besides its lactonase activity, reduces superoxide leakage from the inner mitochondrial membrane (34), thus representing an important defense mechanism against oxidative stress. PON2 also decreases endoplasmic reticulum stress-induced caspase activation (35). We also show an up-regulation of HSP27 and P-HSP27. Wild-type HSP27 lowers the levels of ROS by raising intracellular glutathione (36), whereas P-HSP27 prevents apoptosis interfering with the caspase cascade (33). In addition, HSP27 maintains the stability of actin fibers (37), a function that might be relevant under gravitational unloading to preserve the remaining components of the cytoskeleton.

Besides their own specific function, the common denominator of SIRT2, PON2, SOD2, and HSP27 is their potent antioxidant and antiapoptotic potential. Indeed, despite the marked increase of TXNIP in HUVECs after 10 d in simulated microgravity, we do not observe any accumulation of ROS. Our results suggest that the increased amounts of SIRT2, PON2, SOD2, and HSP27 counterbalance the oxidant action of TXNIP. On the contrary, oxidative stress has been reported in murine fetal fibroblasts and in rat neuronal PC12 cells in simulated microgravity (26, 27) as the result of an imbalance between pro- and antioxidant enzymes. These differences might be due to a more efficient antioxidant arsenal in ECs than in other cell types. In *Caenorhabditis elegans*, an invaluable model that has allowed major advances in our knowledge in many biologic processes, simulated microgravity induces oxidative stress, but also importantly activates the antioxidant defense system in an attempt to reverse the adverse effects of free radicals on nematodes. Therefore, in *C. elegans*, as well as in ECs, both the molecular machineries for the control of oxidative stress and the antioxidant defense system are dysregulated in simulated microgravity.

TXNIP up-regulation is interesting because it confirms what Versari *et al.* (19) described in SPHINX, although limited to RNA level. TXNIP expression is induced by a variety of stresses, including ionizing and exciting radiations, H_2O_2, and mechanical forces (38). In fact, TXNIP acts as a blood flow mechanosensor (39) and is overexpressed when blood flow is disturbed (39). We hypothesize that the alteration of mechanical forces because of microgravity triggers TXNIP up-regulation. In general, TXNIP overexpression renders the cells more susceptible to oxidative stress (40); however, in our experimental model, this is not the case, because we do not detect any increase of ROS or any sign of DNA oxidative damage. As previously mentioned, the pro-oxidant effect of TXNIP is likely to be counterbalanced by the complex and articulated increase of various stress proteins with antioxidant activity. Beyond its role as an endogenous inhibitor of TXR, TXNIP also exerts TXR-independent functions, such as regulation of metabolism and cell growth (41). In HUVECs under stress, TXNIP stimulates the transactivation of VEGF receptor type 2, which is fundamental for endothelial survival (30). It is feasible that TXNIP orchestrates several cellular responses that enable HUVECs to survive microgravity-related stress.

Interestingly, p21 is also increased in HUVECs cultured in the RWV for 10 d. Apart from its role in growth arrest, p21 is induced by a wide range of stress stimuli through p53-dependent and -independent pathways (42). Indeed, p21 exerts a protective action against stress because of its well-described antiapoptotic effects (42).

Our data suggest that the complex and dynamic adaptive response of HUVECs to simulated microgravity contributes to the maintenance of their function. Indeed, we did not detect any alteration in the synthesis and secretion of inflammatory cytokines and chemokines or in the amounts of ICAM-1. NO, crucial to maintain endothelial function (43), was elevated in HUVECs exposed to simulated microgravity for 48 h (8). Here we show that NO is increased after 4 d in the RWV and returns to control levels at d 10.

In general, it is noteworthy that culture in the RWV yields results that closely reflect those obtained in space (19). This consideration raises 2 challenging points. First, it is reasonable to use these bioreactors for benchtop microgravity research to design potentially successful experiments in real microgravity. Second, it is mandatory to study the modulation of proteins in cells cultured in space, because our results clearly demonstrate that, despite no alterations of the levels of transcript, the amounts of the corresponding proteins change. Some evidence has been provided about altered posttranscriptional mechanisms induced by microgravity. By a proteomic approach, it was demonstrated that human T lymphocytes in simulated microgravity down-regulate the 26S proteasome subunit 6 and the proteasome activator complex subunit 3, thus suggesting an impairment of the proteasome machinery (44). Accordingly, culture in the RWV reduced the activity of the proteasome in U937 cells (15). Similarly, a gradual decrease of the total activity of the proteasome was reported in ECs cultured in the RWV for 48 and 96 h (14). More studies are necessary to give new insights into the molecular mechanisms that contribute to cell adaptation.

Briefly, we conclude that early upon exposure to microgravity, HUVECs up-regulates HSP70, which activates a transient adaptive response gradually replaced by the increase of other stress proteins that maintain a new homeostatic status. The sequential up-regulation of different proteins is aimed initially at driving the adaptation to mechanical unloading and finally at establishing and maintaining a novel phenotype that preserves cell viability and function. Fj

ACKNOWLEDGMENTS

This work was supported, in part, by the Italian Space Agency [Coculture of Endothelial Cells and Osteoblast in Space: Effects on Osteoblast Activity (ENDOSTEO) Project]. The authors declare no conflict of interest.

AUTHOR CONTRIBUTIONS

A. Cazzaniga and L. Locatelli performed research; S. Castiglioni and J. A. M. Maier designed research; J. A. M. Maier wrote the manuscript; and all authors analyzed data.

REFERENCES

1. Demontis, G. C., Germani, M. M., Caiani, E. G., Barravecchia, I., Passino, C., and Angeloni, D. (2017) Human pathophysiological adaptations to the space environment. *Front. Physiol.* **8**, 547
2. Najrana, T., and Sanchez-Esteban, J. (2016) Mechanotransduction as an adaptation to gravity. *Front Pediatr.* **4**, 140
3. Baratchi, S., Khoshmanesh, K., Woodman, O. L., Potocnik, S., Peter, K., and McIntyre, P. (2017) Molecular sensors of blood flow in endothelial cells. *Trends Mol. Med.* **23**, 850–868
4. Aubert, A. E., Beckers, F., and Verheyden, B. (2005) Cardiovascular function and basics of physiology in microgravity. *Acta Cardiol.* **60**, 129–151
5. Maier, J. A., Cialdai, F., Monici, M., and Morbidelli, L. (2015) The impact of microgravity and hypergravity on endothelial cells. *BioMed Res. Int.* **2015**, 434803
6. Yee, A., Bosworth, K. A., Conway, D. E., Eskin, S. G., and McIntire, L. V. (2008) Gene expression of endothelial cells under pulsatile nonreversing vs. steady shear stress; comparison of nitric oxide production. *Ann. Biomed. Eng.* **36**, 571–579
7. Carlsson, S. I., Bertilaccio, M. T., Ballabio, E., and Maier, J. A. (2003) Endothelial stress by gravitational unloading: effects on cell growth and cytoskeletal organization. *Biochim. Biophys. Acta* **1642**, 173–179
8. Versari, S., Villa, A., Bradamante, S., and Maier, J. A. M. (2007) Alterations of the actin cytoskeleton and increased nitric oxide synthesis are common features in human primary endothelial cell response to changes in gravity. *Biochim. Biophys. Acta* **1773**, 1645–1652
9. Grenon, S. M., Jeanne, M., Aguado-Zuniga, J., Conte, M. S., and Hughes-Fulford, M. (2013) Effects of gravitational mechanical unloading in endothelial cells: association between caveolins, inflammation and adhesion molecules. *Sci. Rep.* **3**, 1494
10. Griffoni, C., Di Molfetta, S., Fantozzi, L., Zanetti, C., Pippia, P., Tomasi, V., and Spisni, E. (2011) Modification of proteins secreted by endothelial cells during modeled low gravity exposure. *J. Cell. Biochem.* **112**, 265–272
11. Janmaleki, M., Pachenari, M., Seyedpour, S. M., Shahghadami, R., and Sanati-Nezhad, A. (2016) Impact of simulated microgravity on cytoskeleton and viscoelastic properties of endothelial cell. *Sci. Rep.* **6**, 32418
12. Ravagnan, L., Gurbuxani, S., Susin, S. A., Maisse, C., Daugas, E., Zamzami, N., Mak, T., Jäättelä, M., Penninger, J. M., Garrido, C., and Kroemer, G. (2001) Heat-shock protein 70 antagonizes apoptosis-inducing factor. *Nat. Cell Biol.* **3**, 839–843
13. Mariotti, M., and Maier, J. A. M. (2009) Human micro- and macrovascular endothelial cells exposed to simulated microgravity upregulate HSP70. *Microgravity Sci. Technol.* **21**, 141–144
14. Mariotti, M., and Maier, J. A. M. (2008) Gravitational unloading induces an anti-angiogenic phenotype in human microvascular endothelial cells. *J. Cell. Biochem.* **104**, 129–135
15. Maier, J. A. (2006) Impact of simulated microgravity on cell cycle control and cytokine release by U937 cells. *Int. J. Immunopathol. Pharmacol.* **19**, 279–286
16. Hatton, J. P., Gaubert, F., Lewis, M. L., Darsel, Y., Ohlmann, P., Cazenave, J. P., and Schmitt, D. (1999) The kinetics of translocation and cellular quantity of protein kinase C in human leukocytes are modified during spaceflight. *FASEB J.* **13** (Suppl), S23–S33
17. Kapitonova, M. Y., Muid, S., Froemming, G. R., Yusoff, W. N., Othman, S., Ali, A. M., and Nawawi, H. M. (2012) Real space flight travel is associated with ultrastructural changes, cytoskeletal disruption and premature senescence of HUVEC. *Malays. J. Pathol.* **34**, 103–113
18. Kapitonova, M. Y., Kuznetsov, S. L., Froemming, G. R., Muid, S., Nor-Ashikin, M. N., Otman, S., Shahir, A. R., and Nawawi, H. (2013) Effects of space mission factors on the morphology and function of endothelial cells. *Bull. Exp. Biol. Med.* **154**, 796–801
19. Versari, S., Longinotti, G., Barenghi, L., Maier, J. A. M., and Bradamante, S. (2013) The challenging environment on board the International Space Station affects endothelial cell function by triggering oxidative stress through thioredoxin interacting protein overexpression: the ESA-SPHINX experiment. *FASEB J.* **27**, 4466–4475
20. Cotrupi, S., Ranzani, D., and Maier, J. A. M. (2005) Impact of modeled microgravity on microvascular endothelial cells. *Biochim. Biophys. Acta* **1746**, 163–168
21. Dejeans, N., Maier, J. A., Tauveron, I., Milenkovic, D., and Mazur, A. (2010) Modulation of gene expression in endothelial cells by hyperlipaemic postprandial serum from healthy volunteers. *Genes Nutr.* **5**, 263–274
22. Cazzaniga, A., Maier, J. A. M., and Castiglioni, S. (2016) Impact of simulated microgravity on human bone stem cells: new hints for space medicine. *Biochem. Biophys. Res. Commun.* **473**, 181–186
23. Castiglioni, S., Cazzaniga, A., Locatelli, L., and Maier, J. A. M. (2017) Silver nanoparticles in orthopedic applications: new insights on their effects on osteogenic cells. *Nanomaterials (Basel)* **7**
24. Castiglioni, S., Cazzaniga, A., Trapani, V., Cappadone, C., Farruggia, G., Merolle, L., Wolf, F. I., Iotti, S., and Maier, J. A. (2015) Magnesium homeostasis in colon carcinoma LoVo cells sensitive or resistant to doxorubicin. *Sci. Rep.* **5**, 16538
25. Leidi, M., Mariotti, M., and Maier, J. A. (2010) EDF-1 contributes to the regulation of nitric oxide release in VEGF-treated human endothelial cells. *Eur. J. Cell Biol.* **89**, 654–660
26. Wang, J., Zhang, J., Bai, S., Wang, G., Mu, L., Sun, B., Wang, D., Kong, Q., Liu, Y., Yao, X., Xu, Y., and Li, H. (2009) Simulated microgravity promotes cellular senescence via oxidant stress in rat PC12 cells. *Neurochem. Int.* **55**, 710–716
27. Liu, Y., and Wang, E. (2008) Transcriptional analysis of normal human fibroblast responses to microgravity stress. *Genomics Proteomics Bioinformatics* **6**, 29–41
28. Beck, M., Moreels, M., Quintens, R., Abou-El-Ardat, K., El-Saghire, H., Tabury, K., Michaux, A., Janssen, A., Neefs, M., Van Oostveldt, P., De Vos, W. H., and Baatout, S. (2014) Chronic exposure to simulated space conditions predominantly affects cytoskeleton remodeling and oxidative stress response in mouse fetal fibroblasts. *Int. J. Mol. Med.* **34**, 606–615
29. Ballatori, N., Krance, S. M., Notenboom, S., Shi, S., Tieu, K., and Hammond, C. L. (2009) Glutathione dysregulation and the etiology and progression of human diseases. *Biol. Chem.* **390**, 191–214
30. Spindel, O. N., Yan, C., and Berk, B. C. (2012) Thioredoxin-interacting protein mediates nuclear-to-plasma membrane communication: role in vascular endothelial growth factor 2 signaling. *Arterioscler. Thromb. Vasc. Biol.* **32**, 1264–1270
31. Quintá, H. R., Galigniana, N. M., Erlejman, A. G., Lagadari, M., Piwien-Pilipuk, G., and Galigniana, M. D. (2011) Management of cytoskeleton architecture by molecular chaperones and immunophilins. *Cell. Signal.* **23**, 1907–1920

32. Afolayan, A. J., Teng, R. J., Eis, A., Rana, U., Broniowska, K. A., Corbett, J. A., Pritchard, K., and Konduri, G. G. (2014) Inducible HSP70 regulates superoxide dismutase-2 and mitochondrial oxidative stress in the endothelial cells from developing lungs. *Am. J. Physiol. Lung Cell. Mol. Physiol.* **306**, L351–L360
33. Liu, J., Wu, X., Wang, X., Zhang, Y., Bu, P., Zhang, Q., and Jiang, F. (2013) Global gene expression profiling reveals functional importance of sirt2 in endothelial cells under oxidative stress. *Int. J. Mol. Sci.* **14**, 5633–5649
34. Altenhöfer, S., Witte, I., Teiber, J. F., Wilgenbus, P., Pautz, A., Li, H., Daiber, A., Witan, H., Clement, A. M., Förstermann, U., and Horke, S. (2010) One enzyme, two functions: PON2 prevents mitochondrial superoxide formation and apoptosis independent from its lactonase activity. *J. Biol. Chem.* **285**, 24398–24403
35. Horke, S., Witte, I., Wilgenbus, P., Krüger, M., Strand, D., and Förstermann, U. (2007) Paraoxonase-2 reduces oxidative stress in vascular cells and decreases endoplasmic reticulum stress-induced caspase activation. *Circulation* **115**, 2055–2064
36. Vidyasagar, A., Wilson, N. A., and Djamali, A. (2012) Heat shock protein 27 (HSP27): biomarker of disease and therapeutic target. *Fibrogenesis Tissue Repair* **5**, 7
37. Sun, H. B., Ren, X., Liu, J., Guo, X. W., Jiang, X. P., Zhang, D. X., Huang, Y. S., and Zhang, J. P. (2015) HSP27 phosphorylation protects against endothelial barrier dysfunction under burn serum challenge. *Biochem. Biophys. Res. Commun.* **463**, 377–383
38. Han, S. H., Jeon, J. H., Ju, H. R., Jung, U., Kim, K. Y., Yoo, H. S., Lee, Y. H., Song, K. S., Hwang, H. M., Na, Y. S., Yang, Y., Lee, K. N., and Choi, I. (2003) VDUP1 upregulated by TGF-beta1 and 1,25-dihydorxyvitamin D3 inhibits tumor cell growth by blocking cell-cycle progression. *Oncogene* **22**, 4035–4046
39. Spindel, O. N., Burke, R. M., Yan, C., and Berk, B. C. (2014) Thioredoxin-interacting protein is a biomechanical regulator of Src activity: key role in endothelial cell stress fiber formation. *Circ. Res.* **114**, 1125–1132
40. Lane, T., Flam, B., Lockey, R., and Kolliputi, N. (2013) TXNIP shuttling: missing link between oxidative stress and inflammasome activation. *Front. Physiol.* **4**, 50
41. DeBalsi, K. L., Wong, K. E., Koves, T. R., Slentz, D. H., Seiler, S. E., Wittmann, A. H., Ilkayeva, O. R., Stevens, R. D., Perry, C. G., Lark, D. S., Hui, S. T., Szweda, L., Neufer, P. D., and Muoio, D. M. (2014) Targeted metabolomics connects thioredoxin-interacting protein (TXNIP) to mitochondrial fuel selection and regulation of specific oxidoreductase enzymes in skeletal muscle. *J. Biol. Chem.* **289**, 8106–8120
42. Cmielová, J., and Rezáčová, M. (2011) p21Cip1/Waf1 protein and its function based on a subcellular localization [corrected]. *J. Cell. Biochem.* **112**, 3502–3506; erratum: 113, 1450
43. Tousoulis, D., Kampoli, A. M., Tentolouris, C., Papageorgiou, N., and Stefanadis, C. (2012) The role of nitric oxide on endothelial function. *Curr. Vasc. Pharmacol.* **10**, 4–18
44. Risso, A., Tell, G., Vascotto, C., Costessi, A., Arena, S., Scaloni, A., and Cosulich, M. E. (2005) Activation of human T lymphocytes under conditions similar to those that occur during exposure to microgravity: a proteomics study. *Proteomics* **5**, 1827–1837

Received for publication August 1, 2018.
Accepted for publication January 15, 2019.